Aerosol Science and Technology 37: 565–573 (2003)

Published by Taylor and Francis
0278-6826/03/$12.00 + .00
DOI: 10.1080/02786820390126132

Particle Penetration Through Building Cracks

De-Ling Liu[1] and William W. Nazaroff[1,2]
[1]*University of California, Berkeley, California*
[2]*Lawrence Berkeley National Laboratory, Berkeley, California*

Particle penetration into buildings influences human exposure to particles of ambient origin. In this study, we present the results of laboratory experiments measuring particle penetration through surrogates of cracks in building envelopes. Rectangular slots were prepared, with crack heights of 0.25 and 1 mm and flow-path lengths of 4–10 cm, using common building materials: aluminum, brick, concrete, plywood, redwood lumber, pine lumber, and strand board. Air was drawn through a slot from a well-mixed chamber by applying a pressure difference (ΔP) of 4 or 10 Pa. Nonvolatile, electrically neutralized particles were generated and introduced into the chamber. The particle penetration factor was determined, for particle sizes 0.02–7 μm, as the ratio of the particle concentration downstream of the slot to that in the chamber. Particle size and crack height were the two main factors that governed fractional particle penetration. Consistent with prior modeling results, the penetration factor was nearly unity for particles of diameter 0.1–1.0 μm at $\geq$0.25 mm crack height and ΔP of $\geq$4 Pa. Particle penetration diminished for larger and smaller particles and for cracks with significant surface roughness and irregular geometry.

INTRODUCTION

Epidemiological evidence has linked elevated ambient particle levels to adverse human health effects (Pope 2000; Pope et al. 2002). People spend a large proportion of their time indoors (Klepeis et al. 2001). Consequently, human inhalation exposure to particles of outdoor origin depends substantially on the degree to which such particles can penetrate the building envelope and remain suspended in indoor air (Riley et al. 2002).

Buildings are ventilated by three mechanisms. *Mechanical ventilation* is air exchange induced by fans. *Natural ventilation* occurs by wind and buoyancy-induced flow through designed openings in buildings, such as open windows. *Infiltration* refers to the uncontrolled flow of air through cracks and leaks through the building envelope.

In the United States, large commercial buildings commonly have mechanical ventilation systems, and the penetration of ambient particles into these buildings is strongly influenced by the performance of filters in the air handling system (Hanley et al. 1994). In buildings where natural ventilation dominates air exchange, particle penetration should approach unity because the airflow openings are large. Infiltration-dominated air exchange is common in residences, especially when air conditioning or heating is required to maintain thermal comfort. Particle penetration in this case depends on the geometry of the air leakage paths, the pressure difference that induces flow, and particle transport properties. Cumulatively, people spend much time in buildings that are ventilated by means of infiltration. As a consequence, among the particles of ambient origin that are inhaled by humans, a substantial proportion passes through air infiltration pathways of buildings in their transit between source and receptor. A sound understanding of human exposure to airborne particulate matter requires knowledge of the penetration process.

Little was known about particle penetration into buildings until the mid 1990s. Since then, several studies have been published that infer overall particle penetration rates into residences on the basis of model fits to field data on indoor and outdoor particle levels (Thatcher and Layton 1995; Özkaynak et al. 1996; Long et al. 2001; Vette et al. 2001). Other investigators have reported on laboratory-based experiments of particle penetration (Lewis 1995; Mosley et al. 2001). In a prior article, we presented a modeling analysis of particle penetration through single cracks and wall cavities (Liu and Nazaroff 2001). Although these studies have advanced our knowledge, they have not fully elucidated the extent to which particles penetrate building envelopes.

The present paper complements and extends the previous investigations by greatly increasing the quantity of empirical data from laboratory-based experiments. We report on measurements of particle penetration through slots designed to be surrogates of real infiltration pathways in buildings. Most of the slots that we

Received 19 March 2002; accepted 6 February 2003.
This work was supported by the Office of Research and Development, Office of Nonproliferation and National Security, U.S. Department of Energy under contract No. DE-AC03-76SF00098.
Address correspondence to William W. Nazaroff, Department of Civil & Environmental Engineering, University of California, Berkeley, CA 94720-1710, USA. E-mail: nazaroff@ce.berkeley.edu

tested had regular, rectangular geometry, and were made from common building materials. In addition, particle penetration through a broken brick was investigated. The slot dimensions and the applied pressure differences were chosen to be representative of conditions in buildings. Penetration was measured over a broad range of particle diameters, 0.02–7 μm. The results are compared against model predictions (Liu and Nazaroff 2001).

METHODS

Crack Apparatus

Cracks were prepared using seven different materials: aluminum, brick, concrete, plywood, redwood lumber, pine lumber, and strand board. The aluminum plates were machined so that the inner wall surfaces of the crack were apparently smooth (as characterized by touch and profilometry). This represents an idealized case in which surface roughness is expected to have minimal effect on particle deposition. Rectangular slots or cracks were configured from the other six materials by cutting them with conventional methods. Some of the natural surface roughness of these materials was retained to approximately simulate the texture of building cracks. Brick, redwood lumber, and pine lumber were cut to the desired size directly from the original bulk materials. To imitate the coarse surface texture of building gaps made of plywood and strand board, each side of the crack apparatus was created by gluing together several boards, such that the cut ends were exposed to particle-laden airflow with the ply layers oriented in the crossflow direction. For concrete, we made plates by pouring a mixture of Portland cement, sand, and water into a plywood form, so that the surface texture resembled closely that of realistic concrete walls. For wood materials, polyurethane paint and caulking agents were applied on the exterior surface of the crack apparatus to seal the pores, ensuring that air passed through the crack only, and not through the material pores.

The crack apparatus is illustrated in Figure 1. The main component consists of two plates of identical size and materials. In separate experiments, two crack heights, 0.25 and 1 mm, were created by inserting metal shims of the appropriate thickness between the two plates. The crack heights were further confirmed by use of a feeler gauge of appropriate thickness. The crack length, i.e., the dimension parallel to the airflow direction, was 4.3 and 9.9 cm for aluminum cracks, and 4.5 cm for the other materials.

The specific crack heights of 0.25 and 1 mm were selected to represent dimensions of interest for real building leakage paths. The smaller value represents a lower bound of the crack height through which significant infiltration airflow could occur in buildings. For crack heights larger than 1 mm, penetration is expected to be large over a broad range of particle sizes (Liu and Nazaroff 2001).

The crack apparatus was assembled and mounted with a gasket to an aluminum cover that allowed sampling of aerosols flowing through the crack by the measuring instruments. The whole apparatus was coupled to a slot in the wall of a well-mixed aluminum chamber (50 cm $\times$ 40 cm $\times$ 40 cm) into which particles were introduced. A glazing compound was applied to seal leaks at the junction between the crack apparatus and the chamber so that the designed leakage path was the only aerosol flow pathway.

Measuring Penetration

The experimental configurations are illustrated schematically in Figures 2–4. Different arrangements were required for different particle size ranges. In each case, particles were generated and continuously supplied to the aluminum chamber. Air was extracted at a constant rate from the chamber through the crack

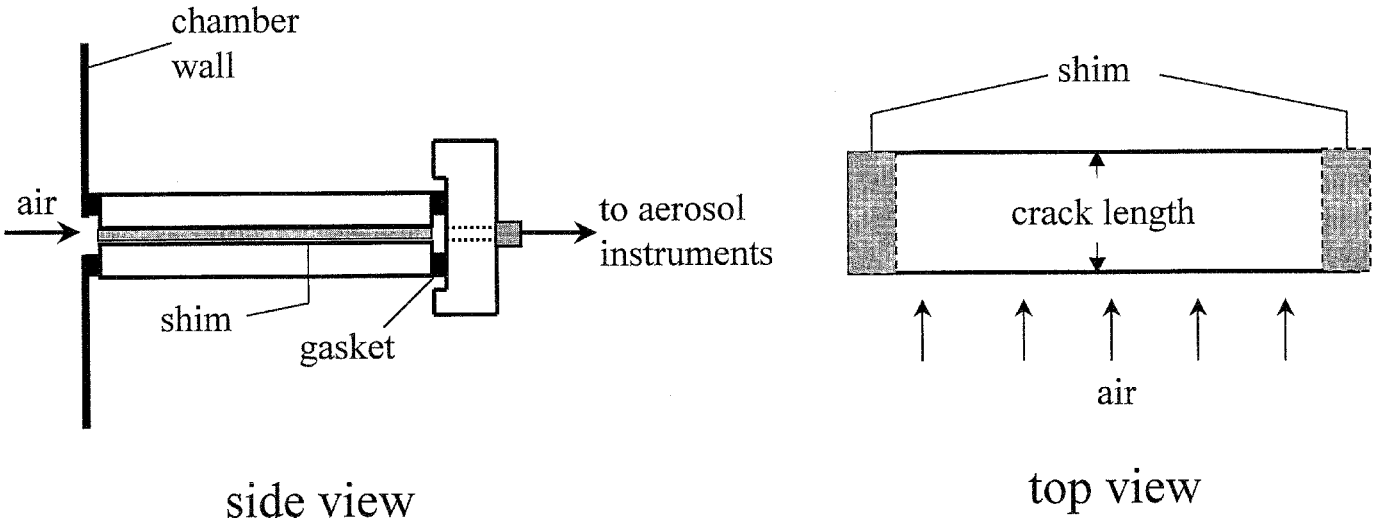

Figure 1. Configuration of crack apparatus (not to scale).

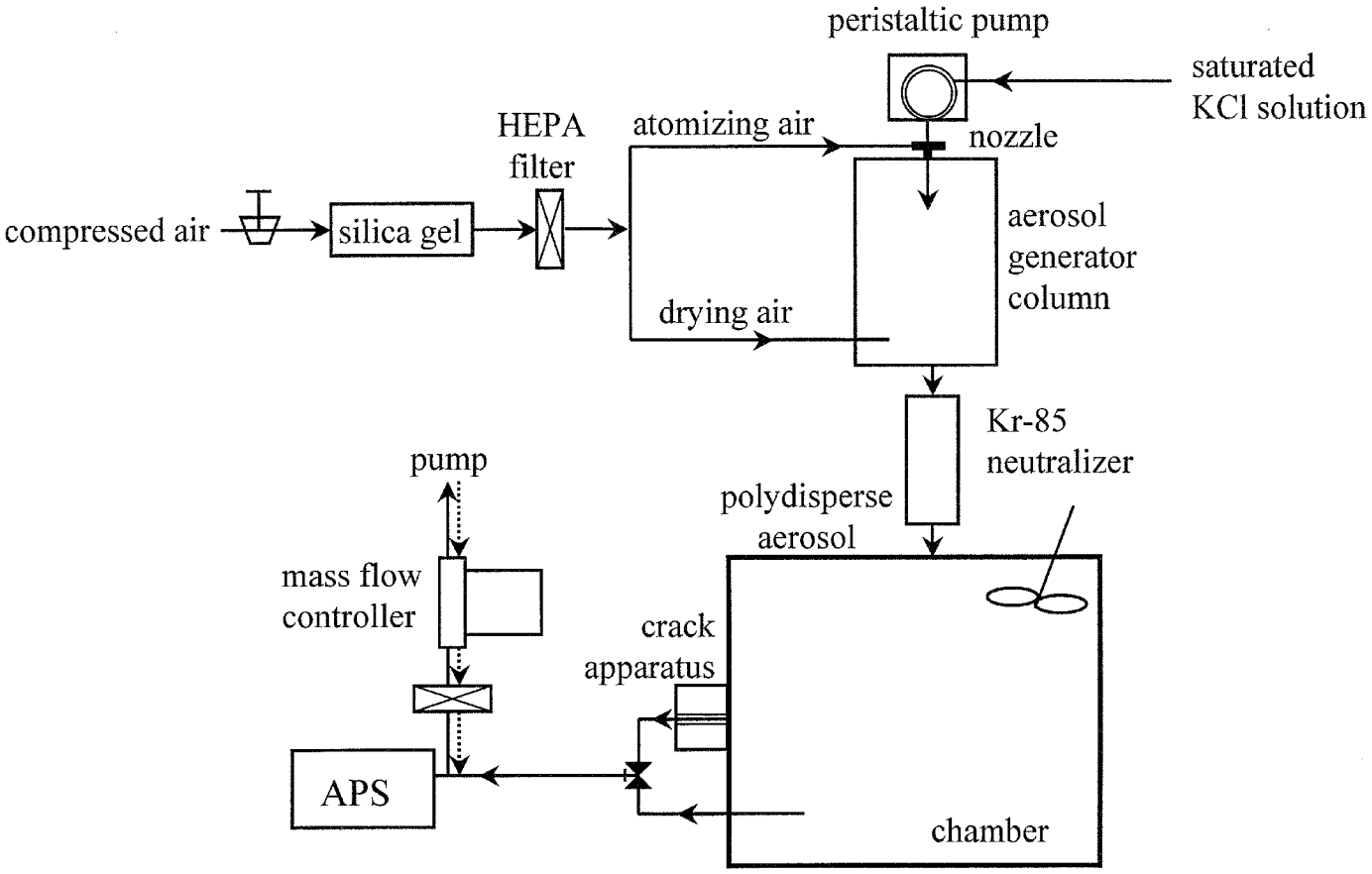

Figure 2. Experimental schematic for measuring particle penetration through the crack apparatus for particle diameter $d_p > 0.6\ \mu$m.

apparatus. Particles were measured upstream and downstream of the crack. The penetration factor was evaluated as the ratio of the downstream to upstream concentration.

For particles larger than 0.6 μm in diameter (Figure 2), polydisperse droplets were generated by supplying a highly concentrated aqueous KCl solution under high pressure into the nozzle of the custom-built atomizer. The spray particles were dried and electrically neutralized before being introduced into the aluminum chamber. For submicron particles (Figure 3), a dilute aqueous KCl solution was supplied to a constant output atomizer (TSI, Inc. Model 3075), and the droplets were then passed through a diffusion dryer and a Kr-85 neutralizer (TSI, Inc. Model 3077). To examine submicron particle penetration with greater precision, experiments were also conducted with monodisperse particles that were generated by means of an atomizer coupled to a differential mobility analyzer (DMA, TSI, Inc. Model 3071), as illustrated in Figure 4. The particle diameters used with this approach were 0.02, 0.03, 0.05, and 0.09 μm.

A pump was employed in conjunction with the aerosol measurement instruments to withdraw air at fixed flow rates out of the chamber so as to maintain the desired pressure difference across the crack ($\Delta P = 4$ or 10 Pa, typical pressure differentials across building envelopes). For the crack sizes and pressure differences that were investigated in this study, the airflow within the crack was laminar. Furthermore, the airflow rate exhibited a linear relationship with pressure difference, indicating that flow resistance was dominated by viscosity (Baker et al. 1987; Chastain et al. 1987). Before each run, the relationship between crack airflow rate and pressure difference was measured. Then, during an experiment, the airflow rate was established at the value necessary to achieve the target value of ΔP.

The particle penetration experiments were performed for particle diameters ranging from 0.02 to 7 μm. Particles were sampled through copper tubing. Two identical tubes (28.4 cm long with an inner diameter of 0.5 cm) were used to connect the chamber and the crack apparatus to a three-way valve. During experiments, the valve was switched to alternately direct the upstream or downstream aerosol flow to one of the measuring instruments (Aerodynamic Aerosol Sizer, APS, TSI, Inc. Model 3320; Electrostatic Aerosol Analyzer, EAA, TSI, Inc. Model 3030; and Condensation Nuclei Counter, CNC, TSI, Inc. Model 3022 or 3022A) (see Figures 2–4). The EAA was used to measure particle number concentrations in seven size ranges, which had mean particle diameters of 0.024, 0.042, 0.075, 0.13,

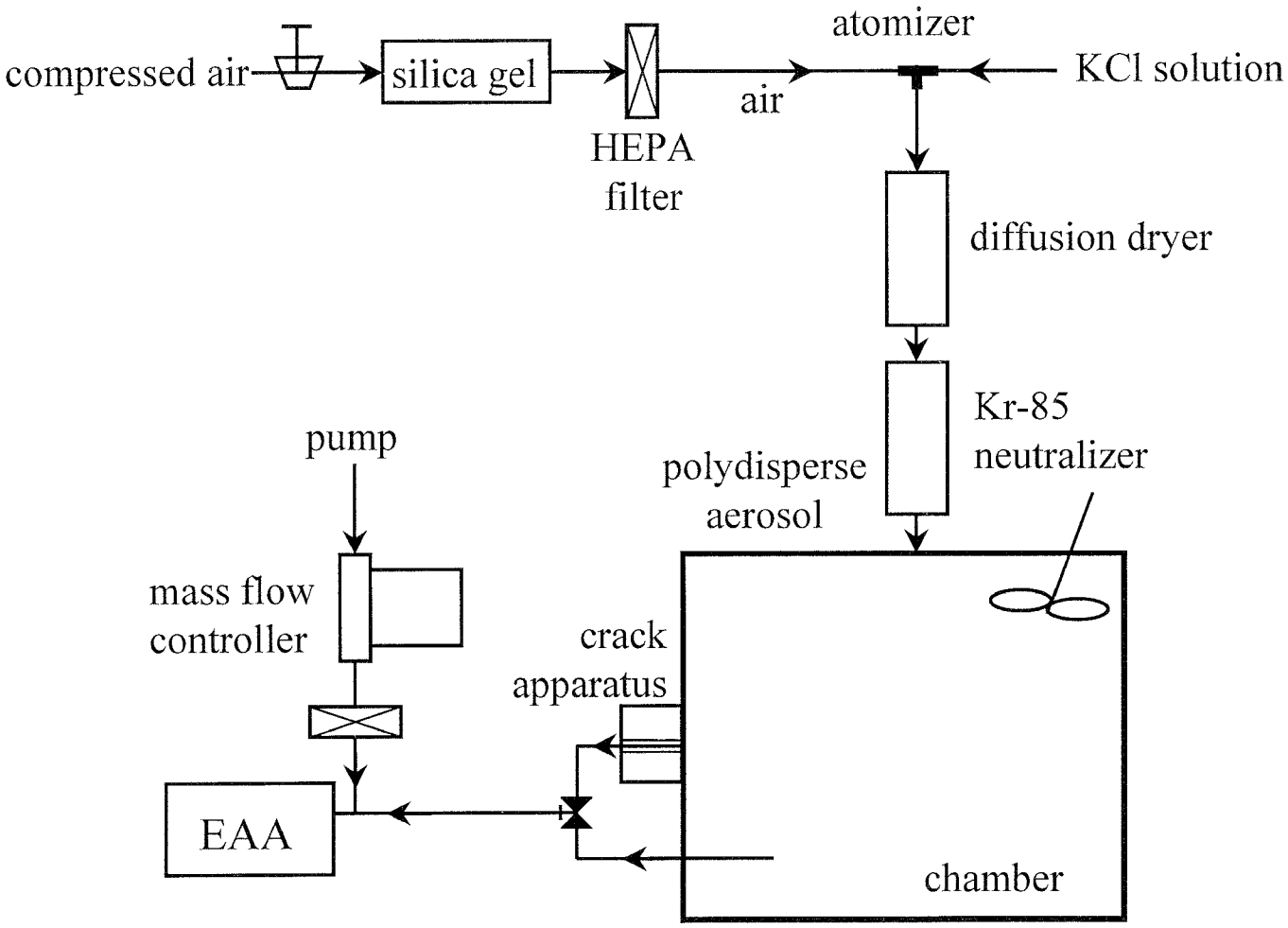

Figure 3. Experimental schematic for measuring particle penetration through the crack apparatus for particle size $d_p < 1$ μm.

0.24, 0.42, and 0.75 μm, respectively. The APS was used to measure size-resolved particle number concentrations for particles larger than 0.6 μm in diameter. For the experiments involving monodisperse particles, the CNC was used to measure particle concentrations.

We began collecting particle concentration data only after the levels in the chamber reached an apparent steady state. Sufficient flushing intervals were used between crack and chamber samples to ensure that our measurements accurately reflected the intended conditions.

RESULTS AND DISCUSSION

Figures 5 and 6 present the experimental results for particle penetration through aluminum cracks under ΔP of 4 and 10 Pa, respectively. The solid and dashed lines in the figures represent the predictions of particle penetration associated with the given crack heights and crack lengths, based on the model for idealized cracks (Liu and Nazaroff 2001). Each symbol in the penetration figures represents the mean value of many measurements for a given particle size. The error bars correspond to ninety-five percent confidence intervals in the mean, based on fluctuations in the measured concentrations. Three data sets are illustrated, with different shapes distinguishing among the three experimental methods.

For a given crack height, the highest particle penetration factors were predicted to occur for particles of 0.1 to 1 μm in diameter. Particles outside of this size range deposit on crack surfaces by means of gravitational settling or Brownian diffusion. The model predictions generally conform well to the experimental results.

The study by Mosley et al. (2001) compared their experimental penetration data to the same modeling predictions, and good agreement was reported. The "total transport fraction" reported by Lewis (1995) was defined as the ratio of the aerosol concentration in a chamber to that of a challenge dust. This fraction combines the effects of particle penetration and deposition to chamber surfaces and so cannot be compared to the penetration results in the present study.

Figure 7 displays the experimental results for cracks made of the six other building materials. Model predictions based on the

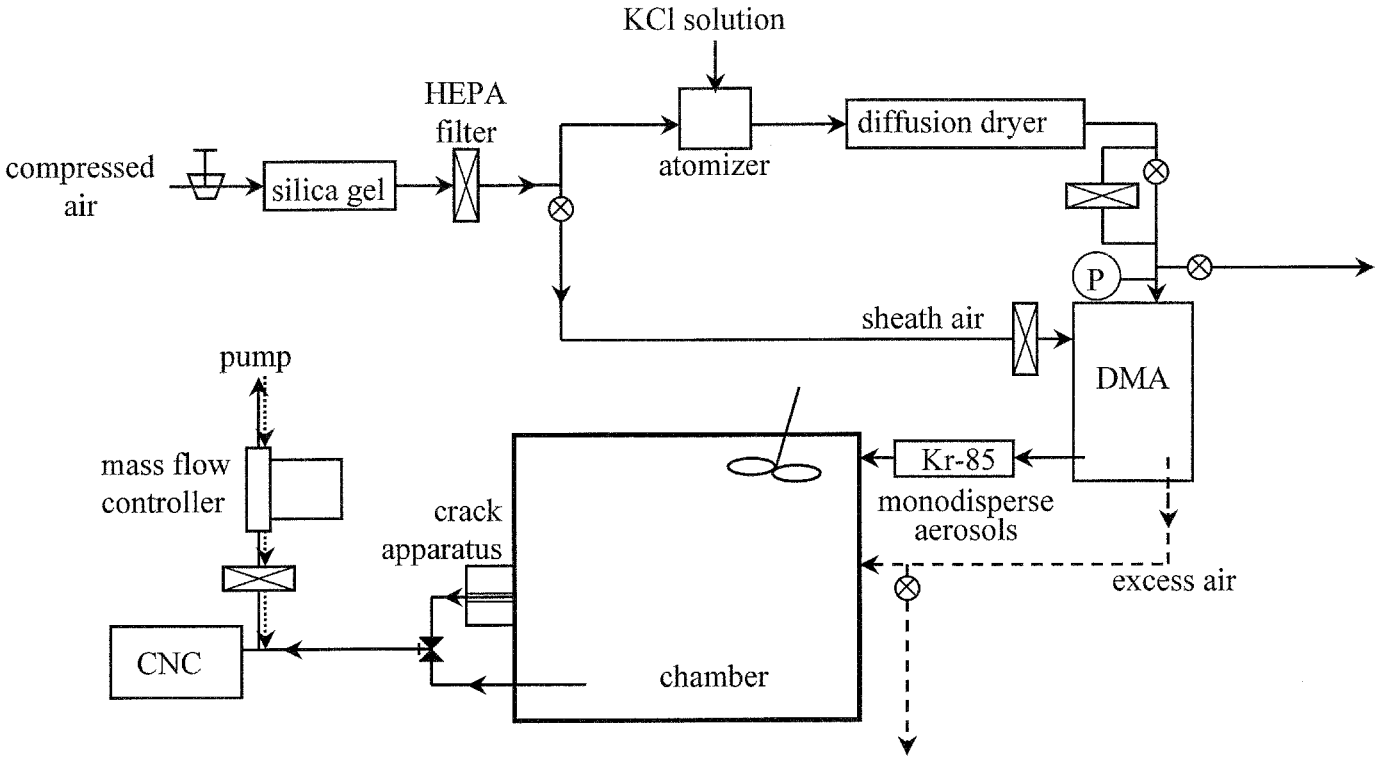

Figure 4. Experimental schematic for measuring particle penetration through the crack apparatus for particle diameter $d_p < 0.1\ \mu$m. (Monodisperse aerosols were generated in this arrangement.)

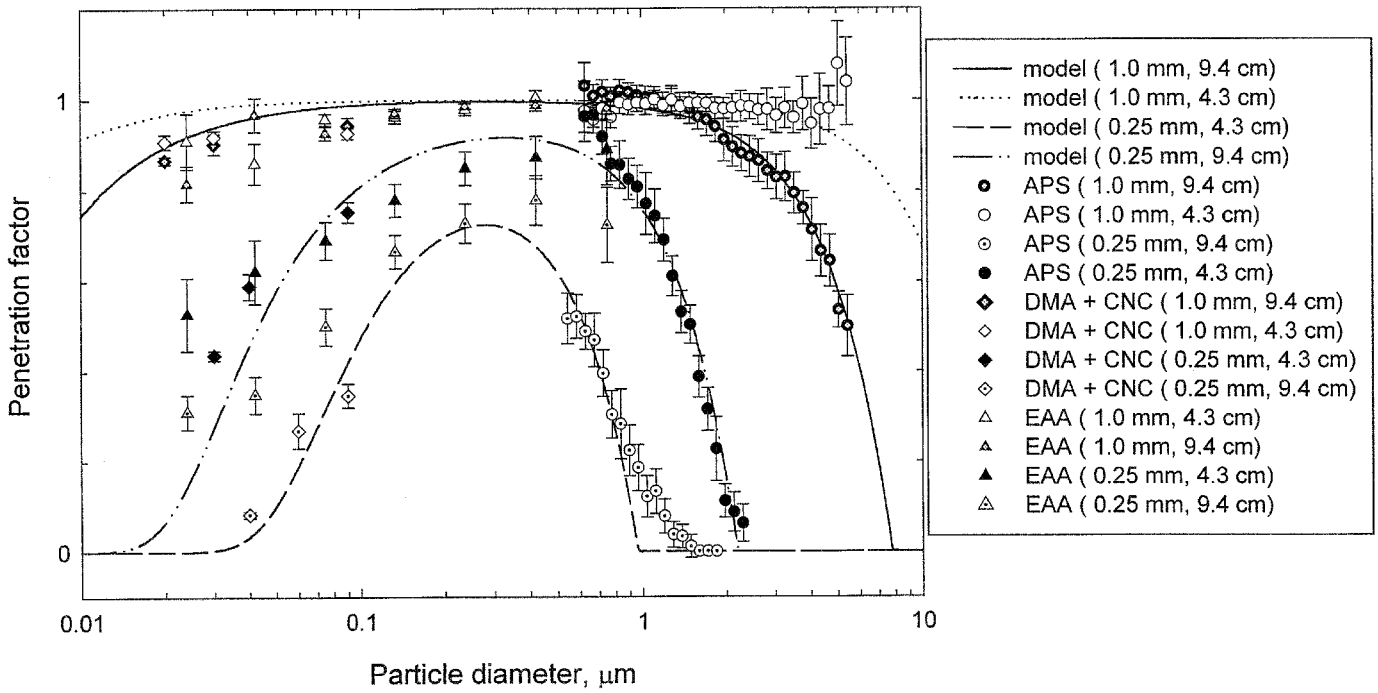

Figure 5. Comparison of model predictions with experimental data for aluminum cracks. Results are presented for four sets of crack dimensions (crack heights of 0.25 mm and 1.0 mm and crack flow lengths of 4.3 cm and 9.4 cm), with an applied pressure difference, $\Delta P = 4$ Pa.

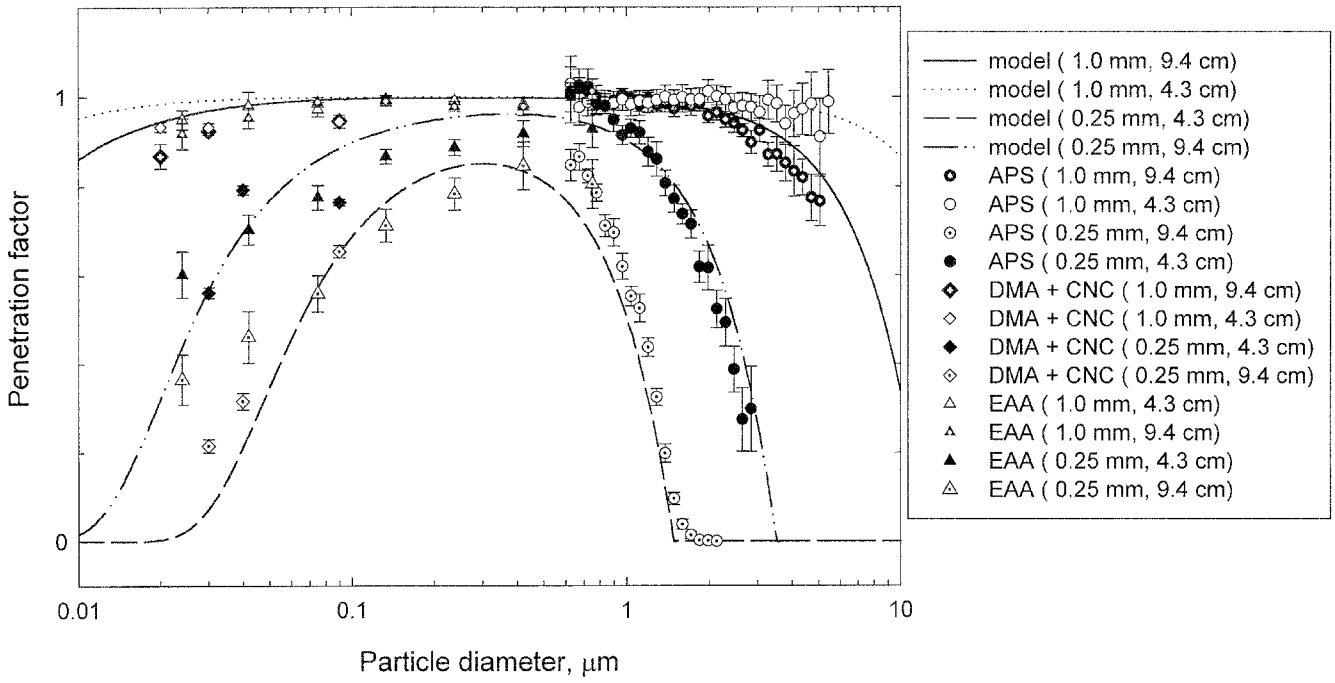

Figure 6. Comparison of model predictions with experimental data for aluminum cracks. Results are presented for four sets of crack dimensions (crack heights of 0.25 mm and 1.0 mm and crack flow lengths of 4.3 cm and 9.4 cm), with an applied pressure difference, $\Delta P = 10$ Pa.

assumption of smooth crack surfaces are also shown. Among the six tested materials strand board and concrete appeared the roughest, based on direct sensory observation (sight and touch). A small piece (200 μm $\times$ 200 μm) of the strand board crack surface was characterized for roughness (Micromap 570 Profiler). The results revealed that the root mean square (rms) height variation along a line was $\sim$15 μm and peak to valley difference was $\sim$70 μm. If a larger area were sampled, these roughness parameters would probably have been larger.

At a crack height of 1.0 mm, the experimental data presented in Figure 7 show essentially complete penetration for all six materials across the full range of particle sizes tested, in good agreement with predictions. For 0.25 mm crack height, penetration was significantly lower, especially for ultrafine (diameter $\leq$ 0.1 μm) and supermicron particles. Moderately good agreement of the model predictions with measurements was observed for most materials.

For redwood and concrete with a crack height of 0.25 mm, deviations are exhibited between model and measurement for particle sizes less than 0.1 μm. We believe that this was caused by deformation of the cracks over time for these two samples, as these experiments were undertaken with a longer delay between fabrication and sampling than were the others. Geometric deviation of the redwood and concrete crack apparatus was confirmed by means of a feeler gauge test, which indicated some lack of uniformity in crack height in the crossflow dimension.

Less particle penetration than predicted was observed in the particle size range of 0.1–1 μm for cracks made of strand board and concrete, where roughness may play a role leading to more particle deposition to crack surfaces. For instance, at a 0.25 mm crack height, for particles in the size range 0.1–0.4 μm, the measured particle penetration factors for these two cracks were less than the predicted values by $\sim$20%. In this size range, Brownian diffusion is an important transport mechanism contributing to deposition in the crack, whereas for larger particles gravitational settling controls the deposition rate. The discrepancy between model and measurement may be a consequence of roughness elements protruding into the particle concentration boundary layer. The boundary layer is thinner for larger diffusive particles, and so roughness is expected to play a greater role in enhancing deposition for 0.1–0.4 μm particles than for ultrafine particles.

We used scale analysis (Bejan 1984) to estimate the particle concentration boundary layer thickness within the crack. At 4 Pa and 0.25 mm crack height, the thickness of the particle concentration boundary layer for 0.03 and 0.3 μm particles was $\sim$370 and 100 μm, respectively. This suggests that the protruding roughness elements on the strand board, for example, may be immersed within the particle concentration boundary layer for ultrafine particles, as illustrated in Figure 8, but extend well into the boundary layer for the case of 0.1–0.4 μm particles. Therefore, for particle diameters less than 0.1 μm, no significant enhancement would be expected for particle deposition in the presence of surface roughness. Also, for particles larger than 0.4 μm, where gravity begins to control deposition, roughness appears to be relatively unimportant, and the smooth-surface model generally conforms well to the experimental data.

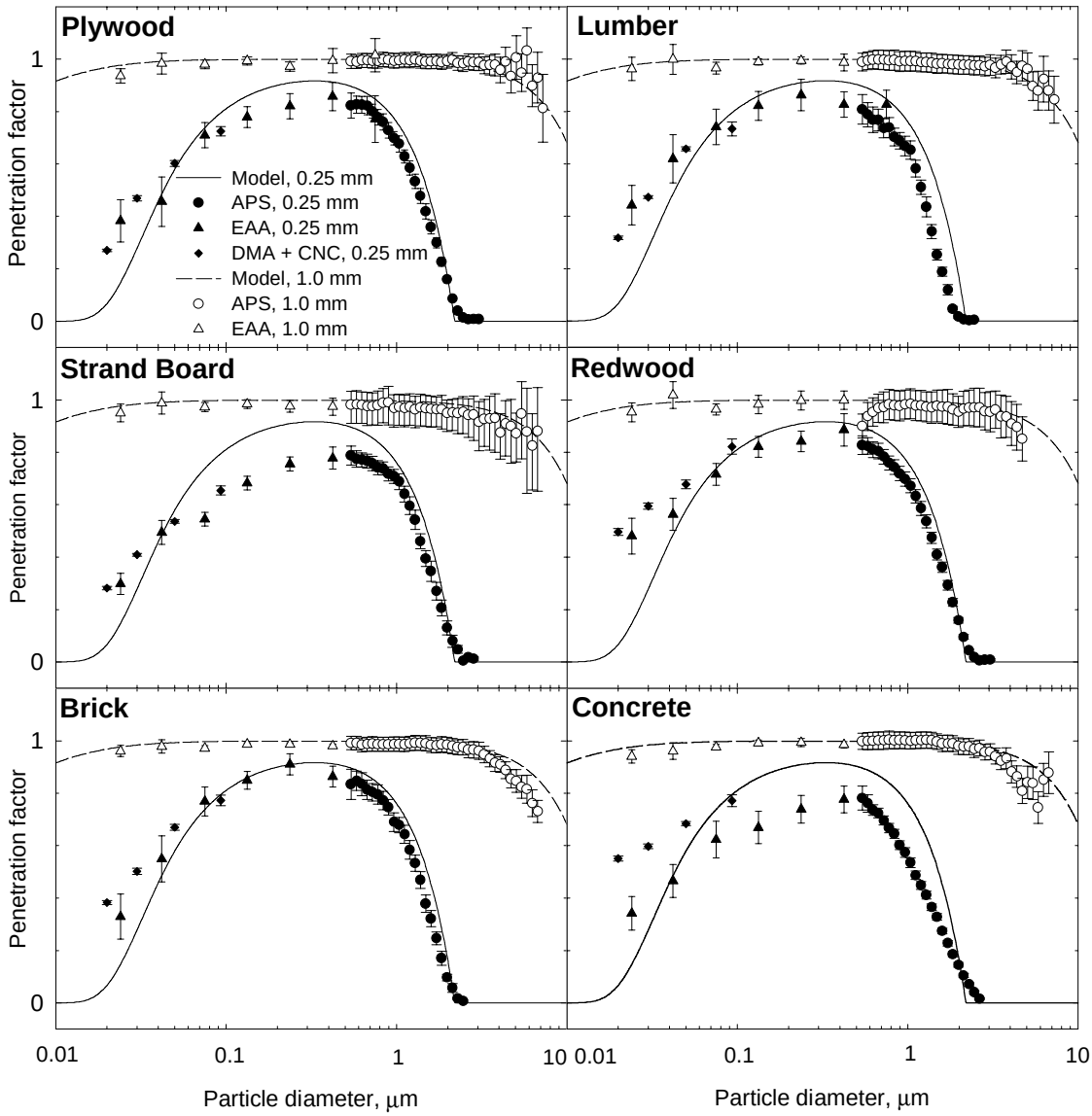

Figure 7. Experimental particle penetration factors for six crack materials at crack heights of 0.25 mm and 1 mm and with $\Delta P =$ 4 Pa, as compared with model predictions.

In addition to surface roughness, the irregular geometry of real cracks may affect particle penetration. To investigate this issue, a real crack, created by breaking a brick, was studied using the same experimental approach. The nominal flow-path length was 4.5 cm. Two crack heights of 0.25 and 1 mm were examined under a pressure difference 4 Pa. In addition to the experimental configurations shown in Figures 2–4, for the crack height of 0.25 mm, an additional approach was required because the aerosol flow rate needed for the target pressure differential was too low to be accurately sampled by the EAA. Instead, a Laser Aerosol Spectrometer (LAS-X, Particle Measurement Systems, Inc., Boulder, CO) was used to determine penetration for 0.1–1 μm diameter particles. Also, to confirm the experimental results measured with the APS, monodisperse particles ($\sim$0.9 μm) generated by a vibrating orifice aerosol generator (VOAG, TSI, Inc. Model 3450) were introduced into the chamber. Particle concentrations from the chamber and downstream of the crack apparatus were measured using a CNC (TSI, Inc. Model 3030).

The experimental results, presented in Figure 9, show generally consistent results among the different measurement techniques. The experimental data for the rough, irregular crack, and the model predictions for a smooth, regular-geometry channel show good agreement for particles smaller than about 0.3 μm diameter. For most larger particle sizes, less penetration was observed than predicted.

Note that at a particle diameter of $\sim$2 μm, the measured penetration did not go abruptly to zero as predicted by the model.

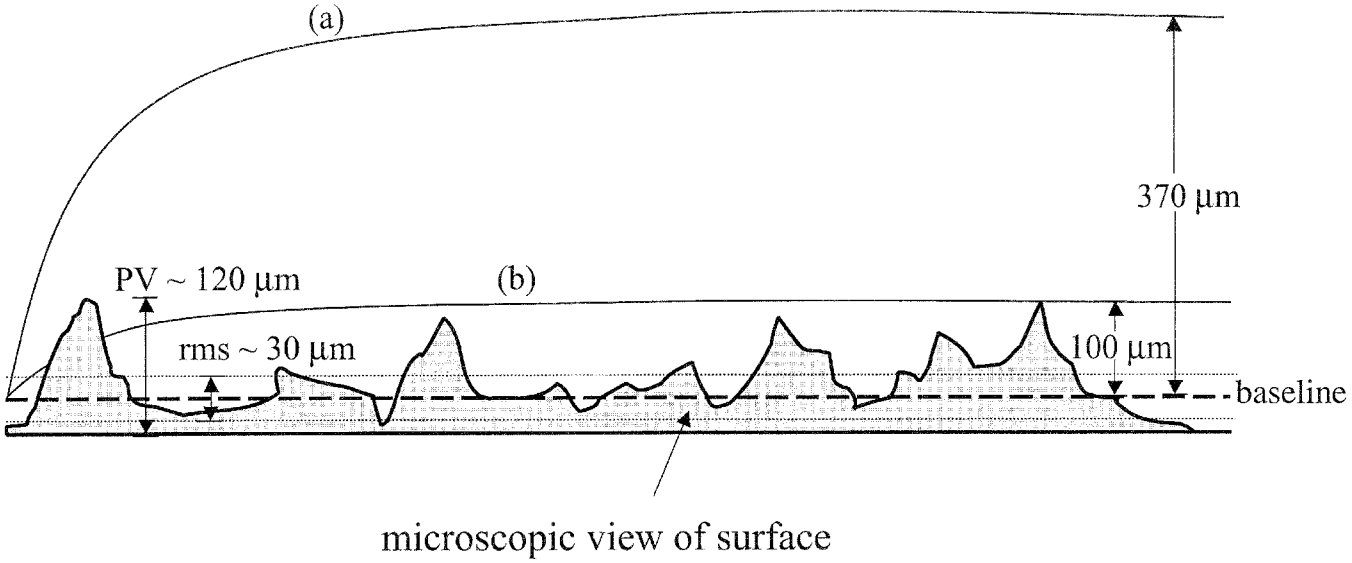

Figure 8. Schematic illustration of concentration boundary layers for particles of (a) 0.03 μm and (b) 0.3 μm. Surface roughness is also illustrated, with rms referring to the standard deviation of the height of the test surface and PV representing the height difference from peak to valley.

A similar result was observed for concrete cracks (see Figure 7), for which the slot openings were not sharp-edged as were other crack samples. A possible explanation for this phenomenon is that certain portions of these irregular flow channels have larger crack heights than the 0.25 mm base value. In the zones with larger crack height, penetration would be more effective than predicted by the model.

For a crack height of 1.0 mm, evident deviations of the experimental data from the idealized predictions occur for supermicron particles. The enhanced deposition of bigger particles might be

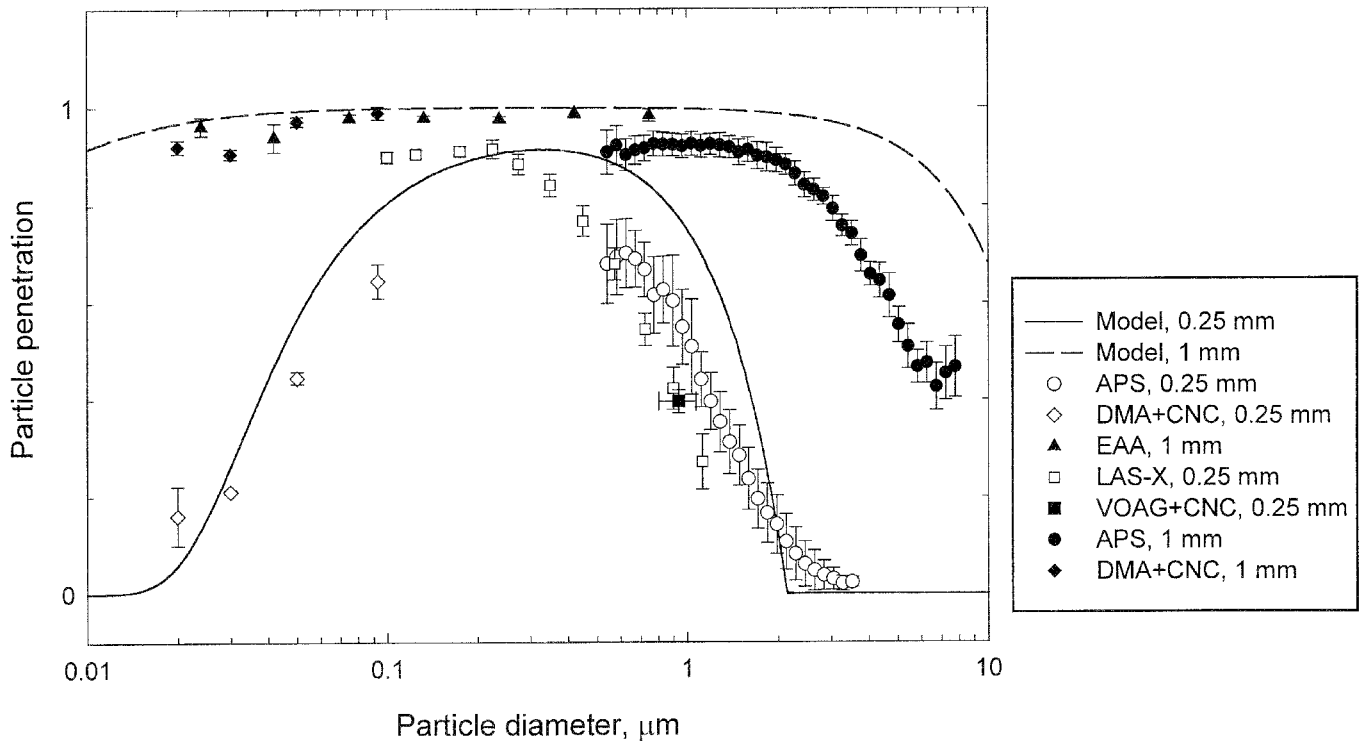

Figure 9. Comparison of model calculations and experimental results for naturally broken brick with crack heights of 0.25 mm and 1 mm.

caused by nonuniform crack geometry that gives rise to local flow irregularity, which in turn leads to impaction or interception when particles hit the protruding elements associated with the rough surfaces. For submicron particles, on the other hand, the experimental data show good agreement with the predictions, suggesting that neither nonuniform crack geometry nor surface roughness has significant influence on particle deposition for this size range.

CONCLUSIONS

The penetration of particles through building envelopes influences human exposure. We believe that a sound understanding of airborne particle penetration through rectangular single cracks, a surrogate of leakage paths in building envelopes, helps shed light on the phenomenon of particle penetration into buildings and the physical factors that affect it. In this paper, we have presented experimental measurements of particle penetration through air leakage paths made of aluminum and a variety of building materials, and compared the results with model predictions formulated for idealized crack configurations. For most cracks with uniform geometry, the experimental particle penetration factors show good agreement with the model predictions, regardless of crack materials. Particle penetration is essentially complete for particles of 0.02–7 μm when the crack height is $\geq$1 mm, and for particle diameters of 0.1–1 μm when the crack height is $\geq$0.25 mm, assuming that the pressure difference is $\geq$4 Pa. The experimental data also indicate that some deviations occur for cracks that exhibit significant surface roughness or irregular channel geometries as illustrated by the strand board, concrete, and natural broken brick.

The work reported here contributes to the base of information about penetration through building envelopes, but additional investigations are needed to fill in important gaps. For example, it would be useful to study particle penetration through real building components, such as windows, which contain a variety of leakage paths. Additional studies in well-characterized single buildings are also needed. Studies published to date have focused on the penetration of nonvolatile particles. Fine particles often contain significant proportions of volatile constituents, such as water, organic compounds, and nitrate. The behavior of such particles and their constituents in air leakage pathways could be considerably different than that of purely nonvolatile particles. Continued developments on this topic would benefit our understanding of how ambient particle sources might affect health. They may also lead us to improvements in building design and operation that reduce human exposure to outdoor particulate matter.

REFERENCES

Baker, P. H., Sharples, S., and Ward, I. C. (1987). Airflow Through Cracks, *Build. Environ.* 22:293–304.

Bejan, A. (1984). *Convection Heat Transfer*, Wiley, New York.

Chastain, J. P., Colliver, D. G., and Winner, P. W., Jr. (1987). Computation of Discharge Coefficients for Laminar Flow in Rectangular and Circular Opening, *ASHRAE Trans*. 27:2259–2283.

Hanley, J. T., Ensor, D. S., Smith, D. D., and Sparks, L. E. (1994). Fractional Aerosol Filtration Efficiency of In-Duct Ventilation Air Cleaners, *Indoor Air* 4:169–178.

Klepeis, N. E., Nelson, W. C., Ott, W. R., Robinson, J. P., Tsang, A. M., Switzer, P., Behar, J. V., Hern, S. C., and Engelmann, W. H. (2001). The National Human Activity Pattern Survey (NHAPS): A Resource for Assessing Exposure to Environmental Pollutants, *J. Exposure Anal. Environ. Epidemiol*. 11:231–252.

Lewis, S. (1995). Solid Particle Penetration into Enclosures, *J. Hazardous Materials* 43:195–216.

Liu, D. L., and Nazaroff, W. W. (2001). Modeling Pollutant Penetration Across Building Envelopes, *Atmos. Environ.* 35:4451–4462.

Long, C. M., Suh, H. H., Catalano, P., and Koutrakis, P. (2001). Using Time- and Size-Resolved Particulate Data to Quantify Indoor Penetration and Deposition Behavior, *Environ. Sci. Technol.* 35:2089–2099.

Mosley, R. B., Greenwell, D. J., Sparks, L. E., Guo, Z., Tucker, W. G., Fortmann, R., and Whitfield, C. (2001). Penetration of Ambient Fine Particles into the Indoor Environment, *Aerosol Sci.Tech.* 34:127–136.

Özkaynak, H., Xue, J., Spengler, J., Wallace, L., Pellizzari, E., and Jenkins, P. (1996). Personal Exposure to Airborne Particles and Metals—Results from the Particle TEAM Study in Riverside, California, *J. Exposure Anal. Environ. Epidemiol.* 6:57–78.

Pope, C. A. (2000). Review: Epidemiological Basis for Particulate Air Pollution Health Standards, *Aerosol Sci. Technol*. 32:4–14.

Pope, C. A., Burnett, R. T., Thun, M. J., Calle, E. E., Krewski, D., Ito, K., and Thurston, G. D. (2002). Lung Cancer, Cardiopulmonary Mortality, and Long-term Exposure to Fine Particulate Air Pollution, *JAMA* 287:1132–1141.

Riley, W. J., McKone, T. E., Lai, A. C. K., and Nazaroff, W. W. (2002). Indoor Particulate Matter of Outdoor Origin: Importance of Size-Dependent Removal Mechanisms, *Environ. Sci. Technol.* 36:200–207 and 1868.

Thatcher, T. L., and Layton, D. W. (1995). Deposition, Resuspension, and Penetration of Particles within a Residence, *Atmos. Environ*. 29:1487–1497.

Vette, A. F., Rea, A. W., Lawless, P. A., Rodes, C. E., Evans, G., Highsmith, V. R., and Sheldon, L. R. (2001). Characterization of Indoor-Outdoor Aerosol Concentration Relationships During the Fresno PM Exposure Studies, *Aerosol Sci. Technol*. 34:118–126.